

# Thioanisole Sulfoxidation by Cytochrome P450<sub>cam</sub> (CYP101): Experimental and Calculated Absolute Stereochemistries

Julia Fruetel,<sup>†</sup> Yan-Tyng Chang,<sup>‡</sup> Jack Collins,<sup>‡</sup> Gilda Loew,<sup>\*,‡</sup> and Paul R. Ortiz de Montellano<sup>\*,†</sup>

Contribution from the Department of Pharmaceutical Chemistry, University of California, San Francisco, California 94143-0446, and Molecular Research Institute, 845 Page Mill Road, Palo Alto, California 94304

Received October 26, 1992. Revised Manuscript Received June 16, 1994<sup>⊗</sup>

**Abstract:** Cytochrome P450 enzymes catalyze three general classes of oxidative reactions:  $\pi$ -bond epoxidations, heteroatom (N, S, P) oxidations, and carbon hydroxylations. Recent work has shown that cytochrome P450<sub>cam</sub> (CYP101) enantioselectively oxidizes styrene and  $\beta$ -methylstyrene and that molecular dynamics calculations predict the enantiomeric specificity with remarkable accuracy. Cytochrome P450<sub>cam</sub> is shown here to also catalyze the stereoselective sulfoxidation of thioanisole (*R:S* 72:28) and *p*-methylthioanisole (*R:S* 48:52). Molecular dynamics calculations suggest that oxidations of thioanisole and *p*-methylthioanisole by cytochrome P450<sub>cam</sub> should yield the corresponding sulfoxides in *R:S* ratios of 65:35 and 22:78, respectively. The predicted and experimental enantiomer ratios for thioanisole change in a similar manner when a *p*-methyl substituent is added to the thioanisole. The theoretical treatment correctly predicts the experimental finding that a *p*-methyl group inverts the preferred sulfoxide stereochemistry.

The oxidations catalyzed by cytochrome P450 enzymes can be broadly classified as hydroxylations, epoxidations, or heteroatom oxidations, although there are oxidative reactions that do not fit neatly into these classifications.<sup>1</sup> The site that is oxidized in substrates that can be oxidized at multiple sites is presumably determined by the intrinsic reactivity of the competing sites, their steric environment, and the orientation of the substrate in the active site determined by protein–substrate interactions. Evidence for competition between sites in a single molecule is provided by the phenomenon of “metabolic switching”, in which substitution of deuterium for hydrogen at one site shifts the hydroxylation reaction to an alternative site.<sup>1,2</sup> It is currently possible, if a mechanism is assumed and orientation factors are negligible, to calculate the relative reactivities of similar sites (e.g., C–H bonds) in a molecule.<sup>3</sup> It has proven very difficult to use computational methods to analyze the effects of substrate–protein interactions, however, because crystal structures are not available for most cytochrome P450 enzymes. One exception to this is cytochrome P450<sub>cam</sub>,<sup>4,5</sup> a soluble, bacterial enzyme which until recently was believed to be highly specific for its normal substrate camphor or molecules closely related to it.<sup>6</sup> The structure of cytochrome P450<sub>cam</sub> in the presence<sup>4a</sup> and absence<sup>4b</sup> of camphor has been solved to a resolution of 1.6 and 2.2 Å, respectively.

Cytochrome P450<sub>cam</sub> has recently been found to be much less substrate-specific than originally thought. For example, cytochrome P450<sub>cam</sub> oxidizes styrene and *cis*- and *trans*- $\beta$ -methylstyrene to the corresponding epoxides,<sup>7a</sup> albeit in processes in which NADH and O<sub>2</sub> consumptions are much less tightly coupled to substrate oxidation than in the case of camphor.<sup>7b</sup> Thus, while camphor turnover results almost exclusively in formation of 5-*exo*-hydroxycamphor, oxidation of the olefins results largely in the production of H<sub>2</sub>O<sub>2</sub> with only a minor fraction of the oxidation equivalents being used for olefin epoxidation.<sup>7b</sup>

The epoxidation of styrene and *cis*- and *trans*- $\beta$ -methylstyrene by cytochrome P450<sub>cam</sub> is stereoselective.<sup>7</sup> This stereoselectivity is determined by interactions between the olefins and the protein that govern the statistical absolute orientation of the olefins in the active site because there is no difference in the intrinsic energies required to oxidize the double bond from the two equivalent faces. The enantioselectivities of styrene and  $\beta$ -methylstyrene epoxidations by cytochrome P450<sub>cam</sub> are therefore well suited for computational analysis. In fact, we demonstrated earlier that the epoxidation enantiospecificity can be predicted with good to excellent accuracy by appropriately designed molecular dynamics simulations.<sup>7</sup> In order to develop a computational approach for the analysis of a second class of oxidation reactions and to explore the general applicability of computational methods to the prediction of stereospecificity, we have extended our investigation to the oxidation of thioanisoles. We report here that cytochrome P450<sub>cam</sub> stereoselectively oxidizes thioanisole and *p*-methylthioanisole and describe a computational method that predicts the experimentally observed stereochemical trend.

## Experimental Section

**Materials.** Thioanisole and *p*-methylthioanisole were purchased from Aldrich Chemical Co. (Milwaukee, WI). Sulfoxide standards were

\* Authors to whom correspondence should be addressed.

<sup>†</sup> University of California, San Francisco.

<sup>‡</sup> Molecular Research Institute.

<sup>⊗</sup> Abstract published in *Advance ACS Abstracts*, November 15, 1994.

(1) Ortiz de Montellano, P. R. In *Cytochrome P450: Structure, Mechanism, and Biochemistry*; Ortiz de Montellano, P. R., Ed., Plenum Press: New York, 1986; pp 217–271.

(2) Foster, A. B. *Adv. Drug Res.* **1985**, *14*, 1–40.

(3) (a) Collins, J. R.; Loew, G. H. *J. Biol. Chem.* **1988**, *263*, 3164. (b) Collins, J. R.; Camper, D. L.; Loew, G. H. *J. Am. Chem. Soc.* **1991**, *113*, 2736.

(4) (a) Poulos, T. L.; Finzel, B. C.; Howard, A. J. *J. Mol. Biol.* **1987**, *195*, 687. (b) Poulos, T. L.; Finzel, B. C.; Howard, A. J. *Biochemistry* **1986**, *25*, 5314.

(5) Cytochrome P450<sub>cam</sub> corresponds to CYP101 in the nomenclature of the following reference: Nebert, D. W.; Nelson, D. R.; Coon, M. J.; Estabrook, R. W.; Feyereisen, R.; Fujii-Kuriyama, Y.; Gonzalez, F. J.; Guengerich, F. P.; Gunsalus, I. C.; Johnson, E. F.; Loper, J. C.; Sato, R.; Waterman, M. R.; Waxman, D. J. *DNA Cell Biol.* **1991**, *10*, 1.

(6) *cam* as substrate-specific enzyme.

(7) (a) Ortiz de Montellano, P. R.; Fruetel, J. A.; Collins, J. R.; Camper, D. L.; Loew, G. H. *J. Am. Chem. Soc.* **1991**, *113*, 3195. (b) Fruetel, J. A.; Collins, J. R.; Camper, D. L.; Loew, G.; Ortiz de Montellano, P. R. *J. Am. Chem. Soc.* **1992**, *114*, 6987.

prepared from the sulfides as described by Rettie *et al.*<sup>8</sup> NADH, catalase, and bis(trimethylsilyl)trifluoroacetamide (BSTFA) were from Sigma (St. Louis, MO). Recombinant cytochrome P450<sub>cam</sub>, putidaredoxin, and putidaredoxin reductase were expressed in *E. coli* and purified as reported.<sup>7b,9</sup> Camphor-free cytochrome P450<sub>cam</sub> was prepared immediately before use by passing it over a Sephadex G-15 column equilibrated with 50 mM potassium phosphate buffer (pH 7.0).

**Product Formation.** A 1 mL volume containing 1  $\mu$ M cytochrome P450<sub>cam</sub>, 8  $\mu$ M putidaredoxin, 2  $\mu$ M putidaredoxin reductase, 5  $\mu$ M catalase (to minimize H<sub>2</sub>O<sub>2</sub>-mediated substrate oxidation), 0.5  $\mu$ L of thioanisole or *p*-methylthioanisole, 0.8 mM EDTA, and 5 mM NADH in 50 mM potassium phosphate buffer (pH 7.0) was incubated at 25 °C for 1 h. The incubation was started by adding the NADH. To quantitate formation of the sulfoxides, 0.2 mL aliquots were removed from the incubation mixtures at designated time points, a solution of the internal standard (*p*-chlorothioanisole) in methanol was immediately added, and the aliquot was extracted with 0.5 mL of CH<sub>2</sub>Cl<sub>2</sub>. The organic layer was analyzed by gas-liquid chromatography on a Hewlett Packard Model 5890A system equipped with a flame ionization detector and interfaced to a Hewlett Packard 3365 Chemstation (DOS series). A DB-1 fused silica capillary column (0.25 mm i.d.  $\times$  30 m) was employed for the analysis. The column temperature was programmed to hold at 100 °C for 4 min and then to rise 10 °C/min to 250 °C and to hold at that temperature for 10 min. The sulfoxides were quantitated using standard curves with *p*-chlorothioanisole as the internal standard. The retention times of the components were as follows: thioanisole, 7.4 min; methyl phenyl sulfoxide, 11.5 min; *p*-methylthioanisole, 9.3 min; methyl *p*-tolyl sulfoxide, 13.5 min; *p*-(hydroxymethyl)thioanisole, 13.9 min; *p*-chlorothioanisole, 10.7 min. The identities of the metabolites were established by coelution with authentic standards by both gas-liquid and high-pressure liquid chromatography and, in the case of *p*-methylthioanisole, by gas-liquid chromatography/electron impact mass spectrometry. To identify the *p*-(hydroxymethyl)thioanisole metabolite, the sample was derivatized with BSTFA.

Mass spectra were obtained on a VG-70 mass spectrometer equipped with a Hewlett Packard 5890A gas chromatograph. The oven temperature was programmed to hold at 120 °C for 2 min, then to increase by 10 °C/min to 250 °C, and finally to hold at 250 °C for 20 min. The retention times of the compounds were as follows: *p*-methylthioanisole, 11.7 min; *p*-methylthioanisole sulfoxide, 19.5 min; *p*-(hydroxymethyl)thioanisole (TMS derivative), 22.3 min.

**Reaction Stoichiometry.** The rates of NADH consumption, oxygen consumption, and hydrogen peroxide formation were determined as previously described except that 5 mM NADH was used for the incubations.<sup>7b</sup>

**Sulfoxidation Stereochemistry.** The ratio of the sulfoxide enantiomers was determined by chiral-phase high-pressure liquid chromatography. A 1 mL incubation mixture of the sulfide incubation mixture described above was extracted with 0.5 mL of CH<sub>2</sub>Cl<sub>2</sub>. The organic layer was then concentrated to  $\sim$ 20  $\mu$ L before it was taken up in 0.25 mL of hexane and injected onto a Chiralcel OB column (4.6 mm i.d.  $\times$  25 cm, Daicel Chemical Industries, Ltd.) in a system consisting of a Hewlett Packard 9153C controller, a Hewlett Packard diode-array detector, and a Varian 9010 solvent delivery system. The column was eluted isocratically at a flow rate of 0.5 mL/min with 80:20 hexane:isopropyl alcohol (thioanisole) and 85:15 hexane:isopropyl alcohol (*p*-methylthioanisole). The eluent was monitored at 254 nm. The retention times of the *S* and *R* sulfoxide enantiomers, respectively, under these conditions are for methyl phenyl sulfoxide, 29 and 47 min, and for methyl *p*-tolyl sulfoxide, 21 and 46 min.

**Theoretical Methodology.** The theoretical methodologies employed here were very similar to those used in our previous study of the stereoselective epoxidations of styrene and  $\beta$ -methylstyrene by cytochrome P450<sub>cam</sub>.<sup>7</sup> First, the lowest energy conformers of thioanisole and *p*-methylthioanisole *in vacuo* were obtained using the semiempirical PM3 method<sup>10</sup> implemented in the program MOPAC (6.0).<sup>11</sup> The Mulliken charge of each atom of these two molecules was then calcu-

**Table 1.** Parameters Added to the AMBER Force Field for Thioanisole and *p*-Methylthioanisole

	Charge <sup>a</sup>		
	thioanisole	<i>p</i> -methylthioanisole	
C1	-0.0770	-0.0756	
C2	-0.0557	-0.0608	
C3	-0.0713	0.0030	
C4	-0.0557	-0.0608	
C5	-0.0779	-0.0766	
H1	0.0556	0.0549	
H2	0.0612	0.0579	
H3	0.0582		
H4	0.0606	0.0573	
H5	0.0579	0.0571	
C3a		-0.1784	
Ha1		0.0608	
Ha2		0.0633	
Ha3		0.0615	
C $\phi$	-0.0334	-0.0376	
S	0.0981	0.0961	
C7	-0.2142	-0.2141	
H71	0.0664	0.0659	
H72	0.0636	0.0630	
H73	0.0636	0.0632	
Bond Parameter <sup>b</sup>			
	$K_r$	$r_{eq}$	
C $\phi$ -S	230	1.773	
Angle Parameter <sup>b</sup>			
	$K_\theta$	$\theta_{eq}$	
C1-C $\phi$ -S	65	120.0	
C5-C $\phi$ -S	65	120.0	
C $\phi$ -S-C7	75	98.0	
Dihedral Parameter <sup>b</sup>			
	$V_n$	$\gamma$	$n$
X-C-S-X	0.8	180.0	2

<sup>a</sup> Charges obtained from STO-3G\* Mulliken populations on PM3-optimized geometries. C1-C5 and H1-H5 denote atoms of the phenyl group that do not connect to the S atom. C $\phi$  is the C atom on the phenyl ring that links to S. C7 is the C atom of the SCH<sub>3</sub> side chain. H3 and C3a are the atoms located at the para position of the phenyl ring. <sup>b</sup> Parameters obtained from CHARM.

lated quantum mechanically with an STO-3G\* basis set<sup>12</sup> using the PM3-optimized geometries. The gaussian  $d$  exponent  $\alpha_d$  for the S atom was chosen to be 0.39. For the subsequent molecular mechanics and molecular dynamics studies with the AMBER programs,<sup>13</sup> a set of empirical parameters which result in minimized substrate geometries consistent with those from PM3, together with the charges from the above *ab initio* calculation, were added to the AMBER force field. Table 1 lists these parameters and charges.

In the next step, both thioanisole and *p*-methylthioanisole were docked in six distinctive orientations in the ferryl form of the cytochrome P450<sub>cam</sub> extended binding site<sup>7</sup> that includes 87 amino acids, seven bound water molecules, the protoporphyrin IX heme unit, and an active oxygen at a distance of 1.7 Å above the Fe. The AMBER all-atom force field was used for all residues except the heme unit, for which the united-atom representation was used. In each initial orientation chosen, the sulfur atom of the substrate was between 3.0 and 3.5 Å from the active oxygen. In three of these orientations, the active oxygen is poised to add to one of the two sulfur lone pairs, leading to the *R* (+), and in the other three, to the second lone pair,

(11) Dewar, M. S. J.; Zoebisch, E. G.; Healy, E. F.; Stewart, J. J. P. *J. Am. Chem. Soc.* **1985**, *107*, 3902.

(12) Collins, J. B.; Schleyer, P. v. R.; Binkley, J. S.; Pople, J. A. *J. Chem. Phys.* **1976**, *64*, 5142.

(13) Singh, U. C.; Weiner, P. K.; Caldwell, J. W.; Kollman, P. A. AMBER UCSF Version 3.0A, Department of Pharmaceutical Chemistry, University of California, San Francisco, 1986. Revision A by George Seibel, 1989.

(8) Rettie, A. E.; Bogucki, B. D.; Lim, I.; Meier, G. P. *Mol. Pharmacol.* **1990**, *37*, 643.

(9) Peterson, J. A.; Lorence, M. C.; Amameh, B. *J. Biol. Chem.* **1990**, *265*, 6066.

(10) Stewart, J. J. P. *J. Comput. Chem.* **1989**, *10*, 209.

**Table 2.** Analysis of the Initial Substrate Orientations<sup>a</sup> and the Interaction Energies of the Optimized Substrate–Enzyme Complex<sup>b</sup>

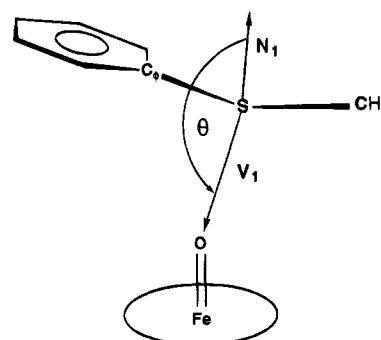
	<i>p</i> -H	CH <sub>3</sub>	<i>r</i> (S–O)	intra	vdW	EES	total int	total <i>E</i>
A. Thioanisole–P450 <sub>cam</sub> Complex								
O1 ( <i>R</i> )	D297,I395	V247,G248	3.15	4.19	–17.57	0.14	–17.44	–3306
O2 ( <i>S</i> )	D297,Q322	L244,D Ring	3.30	4.51	–15.31	0.04	–15.32	–3304
O3 ( <i>S</i> )	F87,Y96	N255,L294	3.40	4.98	–14.13	0.77	–13.36	–3301
O4 ( <i>R</i> )	D297,R299	B ring	3.29	4.25	–17.00	0.15	–16.85	–3308
O5 ( <i>S</i> )	M184,F193	L294,V295	3.40	3.95	–15.68	–0.34	–16.02	–3314
O6 ( <i>R</i> )	M184,F193	A ring	3.24	4.42	–15.07	–0.57	–15.64	–3321
B. <i>p</i> -Methylthioanisole–P450 <sub>cam</sub> Complex								
O1 ( <i>R</i> )	D297,I395	V247,G248	3.23	3.18	–17.25	–0.03	–17.28	–3308
O2 ( <i>S</i> )	D297,Q322	L244,D ring	3.26	3.38	–16.83	–0.40	–17.28	–3308
O3 ( <i>S</i> )	F87,Y96	N255,L294	3.44	3.25	–18.31	–0.01	–18.32	–3309
O4 ( <i>R</i> )	D297,R299	B ring	3.40	3.75	–18.43	0.29	–18.15	–3309
O5 ( <i>S</i> )	M184,F193	L294,V295	3.40	3.14	–16.15	–0.20	–16.35	–3306
O6 ( <i>R</i> )	M184,F193	A ring	3.39	3.74	–15.15	–0.45	–15.60	–3312

<sup>a</sup> The orientation is represented by the residues to which the head (*p*-H or *p*-CH<sub>3</sub>) and the tail (CH<sub>3</sub> that connects to S atom) of the substrate point. The residues are denoted by a one-letter code and their residue number. The A, B, C, and D rings are the four pyrrole rings of the protoporphyrin IX heme unit. The notations A, B, C, and D are based on those used in the crystal structure. <sup>b</sup> The optimized S–O distance in Å is shown in column 4. Intramolecular substrate total energy is shown in column 5. Columns 6–8 list the van der Waals, electrostatic, and total interaction energies between the substrate and the whole enzyme defined in ref 7. The optimized total energy of the complete system is shown in the last column. All energies are in kcal/mol.

leading to the *S* (–) sulfoxide configuration, respectively. These initial substrate dockings are indicated as O1, O2, ..., O6, with the consequent *R/S* product configuration shown in parentheses in Table 2. The longest extension in these substrates is from the *p*-substituent (head) to the methyl group on the sulfur atom (tail). Thus, one way to further specify their orientation, is to indicate to which residues of the binding site each of these two extreme groups of the substrate is pointing. This additional information is given in columns 2 and 3 of Table 2. For example, for thioanisole in the first substrate orientation, O1, the head of the substrate points toward Asp297 and Ile395, while the tail points toward Val247 and Gly248, leading to an *R* (+) configuration. Furthermore, if the substrate backbone is defined as the line from *p*-H or *p*-C through the center of the phenyl ring to the S atom, in the first four complexes, O1–O4, this backbone is approximately parallel to the plane of the heme unit, while in the remaining two orientations, O5–O6, the backbone is perpendicular to it with the *p*-H (or *p*-CH<sub>3</sub>) pointing upward toward Met184 and Phe193.

For each substrate, the six initial substrate–enzyme complexes were minimized and the interaction energies between the substrate and enzyme analyzed, using the AMBER (3.0A) programs. Each optimized complex was then used as the starting configuration for molecular dynamics simulations. Since the 87 amino acids forming the extended binding site are not contiguous, the backbone (N, C<sub>α</sub>, C) atoms of the enzyme were constrained in coordinate space with a harmonic potential of 100 kcal/Å<sup>2</sup> used in the initial set of simulations. In order to examine the effect of this constraint of the enzyme backbone movement on product stereochemistry, a second set of MD simulations was performed for the larger *p*-methylthioanisole substrate, with a reduced backbone harmonic force constant of *k* = 1.0 kcal/Å<sup>2</sup> using orientations O1–O4 and the same initial conditions as for the *k* = 100 kcal/Å<sup>2</sup> simulations. All bonds were constrained using the SHAKE algorithm. Electrostatic interactions were modeled using a distance-dependent dielectric constant with  $\epsilon = r$ . Two different initial velocity distributions corresponding to 298 K were used for each optimized substrate–enzyme complex, resulting in a total of 12 initial conditions from which trajectories were generated for each substrate. For each simulation, a 5 ps heating and equilibration process was performed prior to a 125 ps simulation. The Cartesian coordinates of every atom in the substrate–enzyme complex were stored every 0.2 ps, resulting in 625 coordinate sets per trajectory, or a total of 7500 snapshots.

The criteria that were used to determine the reactivity and product stereochemistry are shown in Figure 1. For each of the 7500 snapshots obtained from the twelve 125 ps simulations, two parameters have been calculated. The first is the distance between the S atom of the substrate and the active ferryl oxygen. Snapshots with S–O distances less than 4.0 Å were assumed to lead to product formation. The second parameter monitored was the face angle  $\theta$ . It is defined as the angle between the normal (N1) of the C–S–C plane and the S to O vector (V1). Values of the angle less than 80° lead to the *S* enantiomer, and

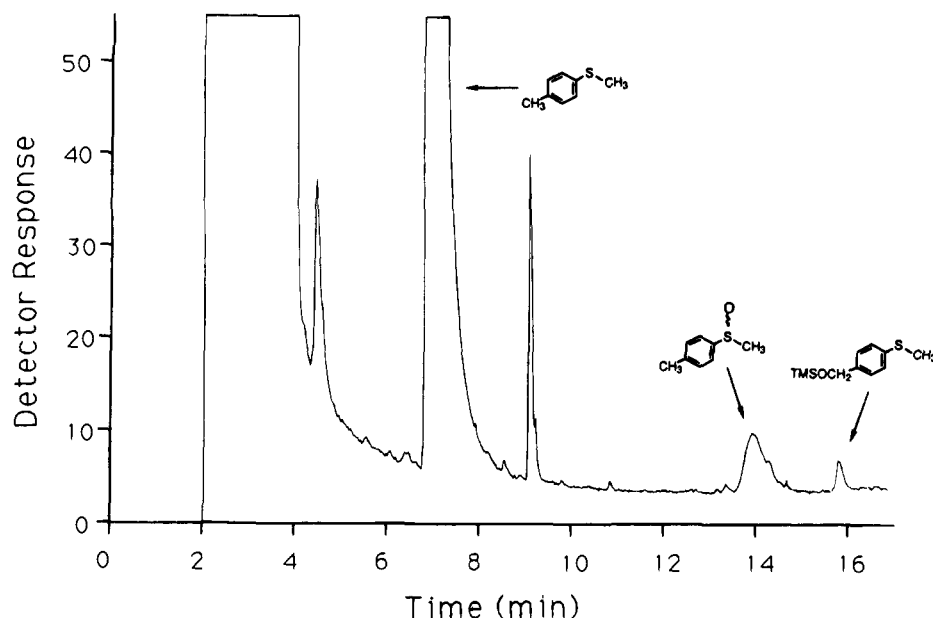


**Figure 1.** Definition of the geometric parameters used to determine the stereochemistries of the sulfoxide products.

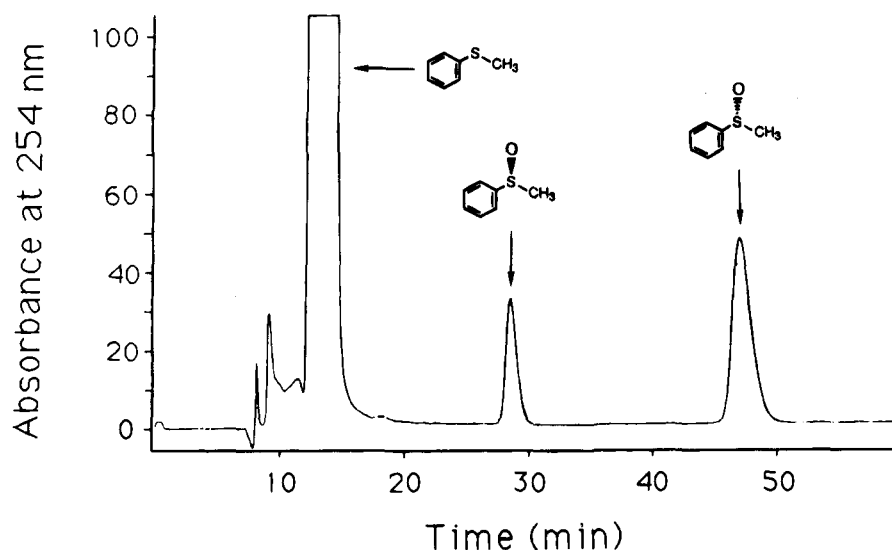
those greater than 100°, to the *R* isomer. Snapshots with values of  $\theta$  between 80° and 100° were disregarded, since they correspond to the transitional configurations between the *R* and *S* isomers.

## Results and Discussion

**Oxidation of Thioanisole and *p*-Methylthioanisole.** Thioanisole and *p*-methylthioanisole are oxidized by a reconstituted, recombinant cytochrome P450<sub>cam</sub> system to the corresponding sulfoxides. The structures of the two sulfoxide products were established by GLC, HPLC, and mass spectrometric comparisons with authentic samples of methyl phenyl sulfoxide and methyl *p*-tolyl sulfoxide (not shown). No product other than the sulfoxide was detected with thioanisole, but a second metabolite is formed in the reaction with *p*-methylthioanisole (Figure 2). The second metabolite elutes very closely to the *S* (–) sulfoxide enantiomer on chiral HPLC using the solvent system employed for determination of the enantiomeric ratio (see below) but can be fully resolved from the sulfoxide peaks by changing the HPLC solvent system. Purification of the second metabolite of *p*-methylthioanisole by HPLC, derivatization with BSTFA, and analysis by gas chromatography–mass spectrometry shows that the trimethylsilylated metabolite has a molecular ion at *m/z* 226, a base peak at *m/z* 137 (loss of OTMS), and a fragment peak at *m/z* 179 (loss of SCH<sub>3</sub>). The higher polarity of the metabolite, its derivatization by BSTFA, and the mass spectrometric properties of the trimethylsilylated product clearly identify it as *p*-(hydroxymethyl)thioanisole. The rates of formation of methyl phenyl sulfoxide and methyl *p*-tolyl sulfoxide (Table 3) are very similar, indicating that the *p*-methyl substituent does not significantly influence the rate of the



**Figure 2.** GLC analysis of the products formed in the incubation of *p*-methylthioanisole with reconstituted, recombinant cytochrome P450<sub>cam</sub>. The GLC conditions are given in the text. The identities of the peaks in the chromatogram are indicated.



**Figure 3.** Chiral-phase HPLC analysis of the enantiospecificity of the oxidation of thioanisole by reconstituted, recombinant cytochrome P450<sub>cam</sub>.

**Table 3.** Comparison of the Rates of NADH and Oxygen Consumption with Those for H<sub>2</sub>O<sub>2</sub> and Product Formation in the Oxidation of Thioanisole and *p*-Methylthioanisole by CytochromeP450<sub>cam</sub>

substrate	turnover (nmol/(nmol of P450/min))			
	NADH	O <sub>2</sub>	H <sub>2</sub> O <sub>2</sub>	sulfoxide
thioanisole	49 (±8)	41 (±5)	48 (±5)	3.5 (±0.5)
<i>p</i> -methylthioanisole	42 (±8)	48 (±5)	37 (±2)	4.0 (±0.5)

reaction (Table 3). These thioanisole sulfoxidation rates are considerably lower than the rate (~260 nmol/(nmol of P450/min)) of hydroxylation of camphor, the normal substrate, but are 3–4 times higher than the rates for the oxidations of styrene and  $\beta$ -methylstyrene.<sup>7b</sup>

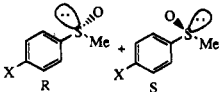
**Stereochemistry of Sulfoxide Formation.** Analysis of the sulfoxide products by chiral HPLC shows that the two phenyl methyl sulfoxide enantiomers are produced from thioanisole in the ratio *R*:*S* = 72:28 (±3) (Figure 3, Table 4). The corresponding ratio for the methyl *p*-tolyl sulfoxide enantiomers produced by cytochrome P450<sub>cam</sub> from *p*-methylthioanisole is *R*:*S* = 48:52 (±1).<sup>14</sup> In both instances, the *S* enantiomer is the

stereoisomer that elutes more rapidly from the chiral-phase HPLC column.<sup>15</sup> Omission of catalase from the incubation mixture decreases the enantiomeric specificity of sulfoxide formation, as expected if the thioanisoles to some extent react directly with H<sub>2</sub>O<sub>2</sub> produced by uncoupled turnover of the enzyme. Catalase was therefore included in all the incubations to more accurately determine the enzymatically-produced sulfoxide enantiomer ratio.

**Reaction Stoichiometry.** Measurements of the rates of NADH and oxygen consumption, and H<sub>2</sub>O<sub>2</sub> and sulfoxide formation, indicate that the majority of the reducing equivalents provided by the NADH are utilized to reduce oxygen to H<sub>2</sub>O<sub>2</sub>

(14) The *R*:*S* enantiomer ratios obtained when the oxidation is catalyzed by cell paste from *Pseudomonas putida* rather than by the purified, reconstituted recombinant enzyme are 39:61 for thioanisole and 19:81 for *p*-methylthioanisole. The purified enzyme isolated from *Pseudomonas putida* gives sulfoxide ratios similar to those produced by the purified, recombinant protein expressed in *E. coli*. The reason for the altered ratios obtained when the cell paste is used is not known, but control experiments suggest that they are not due to further, enantioselective metabolism of the sulfoxides.

(15) Colonna, S.; Gaggero, N.; Casella, L.; Carrea, G.; Pasta, P. *Tetrahedron: Asymm.* **1992**, *3*, 95–106.

**Table 4.** Experimental and Calculated Absolute Stereochemistries of Methyl Phenyl Sulfoxide (X = H) and Methyl *p*-Tolyl Sulfoxide (X = Me)


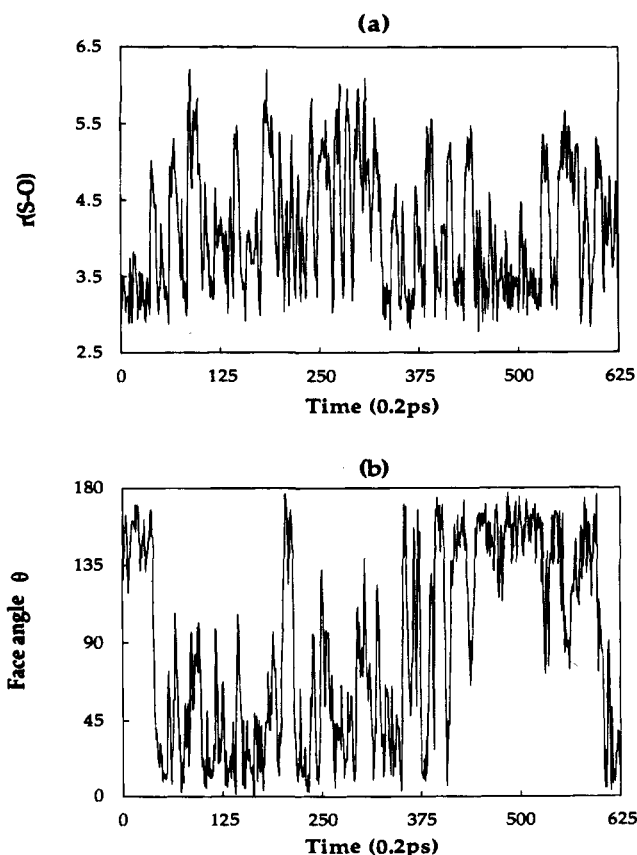
substrate	R:S ratio	
	exptl	calcd
thioanisole	72:28 ( $\pm 1$ )	65:35
<i>p</i> -methylthioanisole	48:52 ( $\pm 1$ )	22:78

rather than to oxidize the thioanisole substrate (Table 3). Sulfoxide formation accounts for only 7–10% of the total NADH turnover. This contrasts sharply with the tight coupling of NADH and oxygen consumption to substrate oxidation in the case of camphor but is reminiscent of the low degree of coupling observed for the catalytic turnover of styrene and *cis*- and *trans*- $\beta$ -methylstyrene.<sup>7b</sup> The comparable values for the consumption of NADH and oxygen and the formation of H<sub>2</sub>O<sub>2</sub> indicate that uncoupling results primarily in peroxide formation and little, if any, reduction of O<sub>2</sub> to water.

**Computation Results.** The optimized geometries of both substrates using the PM3 and AMBER programs (parameters listed in Table 1) are planar. In general, the optimized bond distances and angles are within 0.02 Å and 2° of the known experimental<sup>16</sup> geometries. The rotational barrier about the C<sub>φ</sub>–S bond calculated with AMBER for the side chain SCH<sub>3</sub> is ~2 kcal/mol. The consequence of this low barrier is that the side chain would rotate freely at room temperature and equal *R* and *S* products would be formed if steric interactions with the enzyme did not favor one isomer over the other.

The last six columns of Table 2A,B show the interaction energies of the optimized thioanisole–P450<sub>cam</sub> and *p*-methylthioanisole–P450<sub>cam</sub> complexes, respectively. These interaction energies were examined in order to determine if the energy criterion alone is sufficient to predict the enantiomeric ratios of sulfoxide products. As in the previous theoretical investigation<sup>7</sup> of the epoxidations of styrene and its analogue by cyclochrome P450<sub>cam</sub>, little difference is found among the six distinctive orientations in the substrate–enzyme van der Waals, electrostatic, and total interaction energies.

The two geometrical parameters  $r(S-O)$  and face angle  $\theta$  used to determine the stereochemistry of the sulfoxide products were monitored throughout the simulations. As an example, Figure 4 shows the progression of these two parameters as a function of time for the first trajectory of the thioanisole substrate. The results of each individual 125 ps molecular dynamics simulation for thioanisole and *p*-methylthioanisole are summarized in Table 5, parts A and B, respectively. The notations O1, O2, ..., O6 indicate the initial substrate orientations defined in Table 2, and V1 and V2 denote the two different initial velocity distributions used for each orientation. The predicted sulfoxide stereochemistry, were it to be formed from the optimized substrate–enzyme complex, is shown in the second column. The total number of coordinate sets out of 625 with S–O distances of less than 4.0 Å is listed in the third column. Columns 4–6 show the distribution of snapshots whose face angles lie below 80°, between 80° and 100°, and above 100°, respectively. The ratio of the values in columns 4 and 6 gives the sulfoxide enantiomer distribution, listed in the last column. The overall results yield enantiomeric ratios of

**Figure 4.** Time series plots of  $r(S-O)$  and face angle  $\theta$  for the first trajectory (O1V1) of the thioanisole substrate in the P450<sub>cam</sub> binding site.**Table 5.** Summary of MD Results and the Enantiomeric Ratios for Each 125 ps Trajectory of Thioanisole and *p*-Methylthioanisole<sup>a</sup>

run	conf	total	0–80° (S)	80–100° (R)	100–180° (R)	ratio (R:S)
A. Thioanisole						
O1V1	R	318	141	6	171	55:45
O1V2	R	443	179	11	253	59:41
O2V1	S	394	99	13	282	74:26
O2V2	S	364	134	16	214	61:39
O3V1	S	322	144	6	172	54:46
O3V2	S	419	85	12	322	79:21
O4V1	R	398	100	15	283	74:26
O4V2	R	356	132	12	212	62:38
O5V1	S	11	10	0	1	1:91
O5V2	S	11	6	4	1	14:86
O6V1	R	18	3	10	5	63:37
O6V2	R	55	21	23	11	34:66
total		3069	1035	114	1920	65:35
B. <i>p</i> -Methylthioanisole						
O1V1	R	515	247	3	265	52:48
O1V2	R	451	437	12	2	0:100
O2V1	S	562	549	8	5	1:99
O2V2	S	548	334	6	208	38:62
O3V1	S	535	383	3	149	28:72
O3V2	S	558	534	3	21	4:96
O4V1	R	561	514	8	39	7:93
O4V2	R	557	483	5	69	12:88
O5V1	S	396	250	49	97	28:72
O5V2	S	70	11	18	41	79:21
O6V1	R	438	335	23	80	19:81
O6V2	R	285	13	85	189	94:6
total		5478	4090	223	1165	22:78

<sup>a</sup> The cutoff distance of 4.0 Å for  $r(S-O)$  was used for the results reported here.

sulfoxide products  $R:S = 65:35$  for thioanisole and  $22:78$  for *p*-methylthioanisole. Results from two different cutoff S–O

(16) Zaripov, N. M. *Russ. J. Struct. Chem. (Engl. Transl.)* 1976, 17, 640.

distances, 3.5 and 4.5 Å, were also analyzed to test the sensitivity of the results to the cutoff criterion. For thioanisole, 69:31 (*R*:*S*) and 61:39 (*R*:*S*) ratios were found for the 3.5 and 4.5 Å criteria, both very similar to the 65:35 (*R*:*S*) value for 4.0 Å. For *p*-methylthioanisole, the values of 23:77 (*R*:*S*) and 24:76 (*R*:*S*), respectively, were also very similar to that found for the 4.0 Å cutoff. The result from the molecular dynamics simulation with the smaller backbone harmonic force constant  $k = 1.0 \text{ kcal/Å}^2$  for *p*-methylthioanisole gave a 26:74 (*R*:*S*) ratio of product enantiomers, a ratio very close to that for the  $k = 100.0 \text{ kcal/Å}^2$  simulation.

For these substrates, the results appear to be independent of the minimum S—O distance chosen as a criterion for a reactive configuration of the substrate and of the protein backbone constraint in the binding site model of the enzyme. For thioanisole, in 40% of all configurations monitored, the substrate sulfur atom was close enough to the ferryl oxygen to form a sulfoxide. However, in the two last orientations with the substrate perpendicular to the plane of the heme, only 1–2% of the substrate configurations lead to products. Results from these two orientations do not significantly contribute to the predicted enantiomeric ratio and can be ignored. The remaining eight simulations consistently favor the formation of *R* (+) enantiomers with 60% of all configurations in a reactive mode.

For *p*-methylthioanisole, in contrast, all initial orientations led to simulations in which the substrate is in a reactive mode in a large number of snapshots with an overall value of 73%. However, as for thioanisole, the two perpendicular orientations, particularly O5V2, give the smallest statistics. For this substrate, 9 out of 12 trajectories, as well as the total, strongly favored the *S* (–) sulfoxide.

One of the most interesting results obtained from experiments is the modulation of stereoselectivity from *R* to *S* by the thioanisole *p*-methyl substituent. This qualitative behavior was correctly predicted by the theoretical calculation presented here. However, in terms of the absolute values of the stereoselectivity, a discrepancy between theory and experiment occurs for one of the two substrates. For thioanisole, a fairly good agreement was obtained ( $R:S = 65:35$ , theoretical, and  $R:S = 72:28$ , experimental). On the other hand, the  $R:S = 22:78$  ratio obtained from theory overestimates the preference of the *S* (–) sulfoxide product by 26% for *p*-methylthioanisole compared to the 48:52 ratio from experiment.

In search of the possible sources of this discrepancy, the theoretical method was reexamined and two improvements to the initial approach were made. First, the atomic charges of the substrates were recalculated via a high-level *ab initio* method with the 6-31G\* basis set. Second, the united-atom heme unit was replaced with an all-atom heme. These changes should provide an improved description of the interaction between the substrate and the protein. Molecular dynamics simulations for both substrates were then performed, again using the first four docking orientations described earlier, each with two different velocity distributions. The overall stereoselectivity yielded by the eight trajectories for thioanisole is  $R:S = 57:43$ . This is similar to the  $R:S = 65:35$  ratio from the previous calculation and is still in reasonable agreement with the experiments. For the *p*-methylthioanisole substrate, the same overall stereoselec-

tivity was obtained ( $R:S = 80:20$ ) as in the previous calculation ( $R:S = 78:22$ ). The discrepancy between the theoretical and experimental ratios for this substrate remains. It appears, therefore, that unidentified factors cause the observed discrepancy. In particular, local conformational changes of the residues near the binding site of P450<sub>cam</sub> may occur due to the larger size of the *p*-methylthioanisole substrate that alter the detailed interaction between this substrate and the protein environment. In the current theoretical approach, the starting geometry of the P450<sub>cam</sub> residues was that found in the adamantanone-bound P450<sub>cam</sub> structure and no allowance was made for possible deformation of the local conformation due to the binding of thioanisole and *p*-methylthioanisole. An alternative possibility is that *p*-methylthioanisole has preferred orientations within the P450<sub>cam</sub> binding site. Without knowledge of what these preferred orientations might be, the theoretical study treated all reasonable starting orientations of the substrates equally and the same weight was assigned to them when the resulting sulfoxide product stereochemistries were combined to calculate the predicted isomer ratio. Neither of these factors can be further explored until crystallographic structures of thioanisole- and *p*-methylthioanisole-bound P450<sub>cam</sub> are available.

## Conclusions

Cytochrome P450<sub>cam</sub> enantioselectively oxidizes thioanisole and *p*-methylthioanisole to the corresponding sulfoxides and, to a small extent in the latter case, to *p*-(hydroxymethyl)-thioanisole. The catalytic oxidations of these sulfur compounds are much less tightly coupled to NADH utilization than the oxidation of camphor and result predominantly in the reduction of oxygen to H<sub>2</sub>O<sub>2</sub>. The predicted value for the *p*-methylthioanisole sulfoxide enantiomer ratio from theoretical calculation shifts in the same direction as the observed value although the two values differ in absolute terms. Thioanisole favors *R* (+) sulfoxide formation ( $R:S = 65:35$ , theoretical, and 72:28, experimental) whereas *p*-methylthioanisole favors *S* (–) sulfoxide formation ( $R:S = 22:78$ , theoretical, and 48:52, experimental). The theoretical treatment thus predicts, in agreement with experiment, that introduction of a *p*-methyl substituent leads to an inversion of the preferred absolute stereochemistry of the sulfoxide product. Both the experimental and theoretical results indicate that the *p*-methyl substituent is an important modulator of the stereoselectivity.

**Acknowledgment.** We thank Dr. Allan Rettie for communicating to us his results on the oxidation of thioanisole by cell paste from *Pseudomonas putida*. This work was supported by National Institutes of Health Grants GM25515 (P.O.M.) and GM29743 (G.L.) and Environmental Protection Agency Grant CR818677-01-0 (Y.T.C.). Support for the spectrophotometry and mass spectrometry facilities of the University of California, San Francisco, Liver Center (R. Ockner, Director) is provided by Grant 5 P30 DK26743. The University of California Computer Graphics Facility (R. Langridge, Director) is supported by NIH Grant RR 1081. All calculations were performed on the CRAY YMP at the Pittsburgh Supercomputing Center sponsored by the National Science Foundation.